Multi-Obstacle Avoidance Algorithm for Autonomous Vehicles

Ehab Nossier
Automotive Engineering Department
Faculty of Engineering, Ain Shams University
Cairo, Egypt
ehab.nossier@eng.asu.edu.eg

Fady Ibrahim
Automotive Engineering Department
Faculty of Engineering, Ain Shams University
Cairo, Egypt
fady.ibrahim@eng.asu.edu.eg

M. Abdelwahab
Automotive Engineering Department
Faculty of Engineering, Ain Shams University
Cairo, Egypt
mohamed_abdelwahab2010@eng.asu.edu.eg

M. AbdelAziz
Automotive Engineering Department
Faculty of Engineering, Ain Shams University
Cairo, Egypt
mohamed_abdelaziz@eng.asu.edu.eg

***Abstract*— This paper presents a local path planning approach that avoids both static and dynamic multi-obstacles for autonomous car. The proposed algorithm is able to alter the predefined waypoints from global path planning when obstacles are detected. A set of paths are generated based on the sigmoid function for overtaking obstacles. Every single path is assessed according to a cost function which includes path safety, comfortability, and length. Genetic algorithm is used to optimize parameters of the selected sigmoid function for smoothness and minimum length. Non-linear Model Predictive Controller is designed for trajectory tracking considering vehicle's dynamics. Simulation results reveal that the algorithm carries out obstacle avoidance and can handle multi-obstacles furthermore, the lateral acceleration is reduced by 44.27% and 50% in both static and dynamic scenarios effectively.**

Keywords*— *Path Planning, Sigmoid Function, Multi obstacle avoidance, Genetic Algorithm, Non-linear Model Predictive Control.

I. Introduction

Intelligent mobility nowadays is a crucial research field for all vehicle manufacturers. There is intense rivalry between companies to alter the vehicle to ego-vehicles without the necessity of drivers. Every year worldwide, 1.35 million people die in road death, with more than 50 million people suffering life-threatening injuries [1]. In Egypt, 9.7 per 100,000 road deaths every year with almost 10,000 in serious injuries [1]. According to the statistics, human negligence is the cause of more than 90% of road accidents [1]. Autonomous vehicles are playing a vital role to increase road safety, which results in enhancing productivity.

Besides, there are numerous studies in recent years on both static and dynamic path planning. Path planning aims to extend the ego-vehicle with a safe collision-free path to the desired destination, taking into consideration the vehicle dynamics. Global and local path planning are the two phases of path planning algorithms. The global path planning approach is to ascertain a route with a prior known environment obtained from maps and localization systems from an initial position to a target position. The widely used approaches for global planning are Dijkstra, A*, D*, and Rapidly exploring Random Tree RRT [2-5]. These algorithms obtain an optimal path from one position to another. Nevertheless, these algorithms are slow, time consuming, and output paths are not continuous, thus not appropriate for real-time applications [6].

The local path planning is achieved by altering the global route when an obstacle is detected by sensors in the perception stage. For instance, polynomial curves were used by Petrov and Nashashibi [7] for overtaking maneuvers in real-time applications excluding any prior knowledge of the overtaken vehicle speed. In [8] The approach is based on Bezier curves and circumference parametric equations for path generation. The results showed that the computational time is reduced in the tracking stage. In [9] proposed a new approach for obstacle avoidance using aesthetic B-spline curves with minimal and short paths, and the results showed that the approach is feasible and satisfies comfortability. Cubic spline path planning was presented in [10] by generating a constant set of path candidates. Then the optimal path is selected based on a cost function nevertheless, the algorithm deals only with one moving obstacle. Support vector machines (SVM) is used in [11]. The algorithm combines SVM with a particle filter to predict moving obstacles in an unstructured environment. In [12] presented a path planning algorithm based on a modified sigmoid function, however, the algorithm deals only with a single obstacle and the function parameters were imposed. In [13] introduced a local path planning method based on sigmoid function taking into account relative speeds. The algorithms can handle situations when the front vehicle accelerates, but the algorithm is only used for a single preceding vehicle.

In addition, path tracking plays a vital role in intelligent mobility. Different types of controllers are used in path tracking. In [14] used predictive Stanley and the results revealed that the controller minimizes the lateral error by 53% and yaw stability by 22% than basic Stanley. In [15] proposed a NMPC which followed effectively the reference path with minimum error while maintaining comfortability for passengers. In [16] proposed Z-Number Based Fuzzy Logic control to achieve robust and generalizable performance. In [17] proposed an adaptive discontinuous posture controller to track a set of waypoints in a smooth path.

In this paper, a multi obstacle avoidance algorithm is proposed, where a local path planning approach based on sigmoid function is presented, which handles both single and multi-obstacles instead of a single obstacle presented in

2021 16th International Conference on Computer Engineering and Systems (ICCES) | 978-1-6654-0867-7/21/$31.00 ©2021 IEEE | DOI: 10.1109/ICCES54031.2021.9686134

[11,12,13], while (NMPC) is designed for trajectory tracking considering vehicle's dynamics.

This paper consists of 4 sections besides the introduction. Section 2 introduced the path planning approach for overtaken maneuvers. Section 3 presents the implementation of the path tracking NMPC with the vehicle dynamic model. In Section 4, the simulation results are presented. Finally, conclusions are drawn in Section 5.

II. Path Planning Approach

The proposed path planning method is based on the sigmoid function to avoid multi obstacles. When obstacles are detected, the algorithm alters online the initial trajectory from the global planner to ensure a safe and comfortable path to overtake the passing vehicles or pedestrians with low execution time. The proposed method aims to handle both static and dynamic obstacles furthermore deal with multi-obstacles different from the proposed methods in [12,13]. Furthermore, the generated path is proportional to the number of obstacles detected without the necessity of generating a constant set of paths.

A. Path Generation

The generated path is based on a mathematical sigmoid function that added a lateral veer to a straight path. As shown from Fig. 1. the sigmoid function graph is similar to lane-change manoeuvres.

$$y1(x) = \frac{1}{1+e^{-x}} \tag{1}$$

$$y2(x) = \frac{-1}{1+e^{-x}} \tag{2}$$

The modified sigmoid function is presented in [11].

$$Y_r = \sqrt{S^2 - (X(N) - X_{obstacle})} + Y_{obstacle} \tag{3}$$

$$\mathrm{Y(N)} = \frac{Y_r}{\left(1+e^{(C(d(N)-Sm))}\right)} \tag{4}$$

Where, S lateral safety offset distance, ($X_{obstacle}$, $Y_{obstacle}$) detected obstacle position, d(N) Euclidean distance between the global path trajectory and the obstacle position, C is the smoothness coefficient (C ∈ [0 1]) and Sm longitudinal safety distance. As shown from Fig. 2. the initial path is modified when a vehicle is detected.

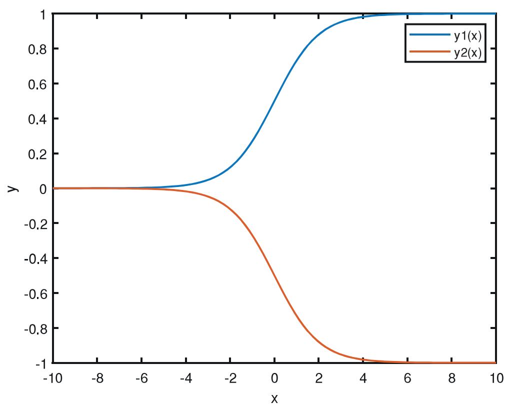

Fig. 1. Sigmoid function curve.

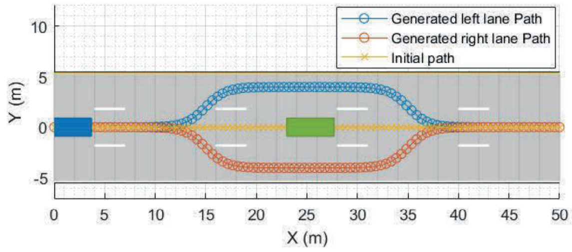

Fig. 2. Path generation when a vehicle is detected.

The proposed algorithm generates two paths for each vehicle to perform right or left overtaking maneuvers furthermore, two additional paths involving minimum Euclidean distances for the detected vehicles.

B. Path Selection and Optimization

When obstacles are detected, thus generating series of path candidates. Every single path is assessed for safety distance between Ego-Vehicle and other vehicles. If a collision is detected or the vehicle-vehicle distance is smaller than the safety distance, the path is terminated. Furthermore, the remaining paths are evaluated for safety, path length, and smoothness. A cost function is carried out for the paths then the best path is achieved by minimizing the total cost function in equation (5).

The total cost function is defined as:

$$cf(N_p) = w_s * cf_s(N_p) + w_{pl} * cf_{pl}(N_p) + w_{sm} * cf_{sm}(N_p) \tag{5}$$

Where cf is the total cost function. cf_s, cf_{pl} and cf_{sm} are the cost functions for safety, path length, and smoothness, respectively for the cost function. w_s, w_{pl} and w_{sm} are the weights and their value influences the driving behaviour. Increasing w_s results in a safer but longer path, while increasing w_{pl} results in a shorter path. In this study, the weights are set to 0.5, 0.3, and 0.2, respectively. The weights are set based on the highest priority to safety to ensure a collision-free path and keep a vehicle-to-vehicle safety distance along the path. Path length and smoothness weights are set to keep the lateral acceleration on the comfort level, thus minimizing side slip on maneuvers. The selected path is optimized using a genetic algorithm [18]. Consequently, the three variables are obtained from the first-time step with the population size is set to 50 and the maximum number of iterations is 50. The optimization is carried out for the three variables (C, S, Sm) in equations (3,4). Where C ∈ [0,1], S ∈ [3,5] and Sm ∈ [5,10].

III. PATH TRACKING

The NMPC is used for path tracking. The MPC formulation is considered as follows:

$$min_{u(t)}\{ J = \int_{t_0}^{t_f} \big(x(t), u(t)\big) dt \}$$

Subject to:

$$\dot{x}(t) = f(x(t), u(t), p, t)$$
$$x(t_0) = x_0$$
$$x_{min} \leq x_i(t) \leq x_{max}$$
$$u_{min} \leq u_i(t) \leq u_{max}$$
$$t \in [t_0, t_f]$$

where x(t) $\in \mathbb{R}^{n_x}$ represents state variables vector. And x(t) $\in \mathbb{R}^{n_u}$ is the control input vector. the time-independent parameters are defined as p $\in \mathbb{R}^{n_p}$. The initial state x(t_0) is known. The time horizon is defined as t $\in$ [t_0, t_f] where initial time t_0 and final time t_f.

In this paper, 3DOF for 4-wheel vehicles presented in [19-20] are used and stated as follows:

$$ma_x = F_{x,fr}\cos(\boldsymbol{\delta}) + F_{x,fl}\cos(\boldsymbol{\delta}) - F_{y,fr}\sin(\boldsymbol{\delta}) - F_{y,fl}\sin(\boldsymbol{\delta}) + F_{x,rr} + F_{x,rl} - TR \quad (6)$$

$$ma_y = F_{x,fr}\sin(\boldsymbol{\delta}) + F_{y,fr}\cos(\boldsymbol{\delta}) + F_{x,fl}\sin(\boldsymbol{\delta}) + F_{y,fl}\cos(\boldsymbol{\delta}) + F_{y,rr} + F_{y,rl} \quad (7)$$

$$I_z * \dot{\omega}_z = (F_{x,fr}\sin(\boldsymbol{\delta}) + F_{y,fr}\cos(\boldsymbol{\delta})) * lf + \big(F_{x,fl}\sin(\boldsymbol{\delta}) + F_{y,fl}\cos(\boldsymbol{\delta})\big) * lf - F_{x,fr}\cos(\boldsymbol{\delta}) * \frac{B_f}{2} + F_{x,fl}\cos(\boldsymbol{\delta}) * \frac{B_f}{2} + F_{y,fr}\sin(\boldsymbol{\delta}) * \frac{B_f}{2} + F_{y,fl}\sin(\boldsymbol{\delta}) * \frac{B_f}{2} - F_{x,rr} * \frac{B_r}{2} + F_{x,rl} * \frac{B_r}{2} - F_{y,rr} * lr - F_{y,rl} * lr \quad (8)$$

Where a_x, a_y are the longitudinal and lateral acceleration respectively, $\boldsymbol{\omega}_z$ yaw acceleration,

m, I_z are the mass and moment of inertia of the vehicle. $F_{x,i}$ are the longitudinal wheel forces, $F_{y,i}$ are the lateral wheel forces (*i=fl, fr, rl, rr*) respectively and $\boldsymbol{\delta}$ is the steering angle of the front wheels. l_f, l_r are the front and rear wheelbase, respectively. B_f, B_r are front and rear track, respectively. The acceleration terms acan be computed as follows:

$$a_x = \big(\dot{v}_x - v_y * \omega_z\big) \quad (9)$$

$$a_y = \big(\dot{v}_y + v_x * \omega_z\big) \quad (10)$$

TR is the total resistances, R_R is the rolling resistance, R_{air} aerodynamic resistance, R_G gradient resistance.

$$TR = R_R + R_{air} + R_G \quad (11)$$

$$R_R = f_r * w * \cos(\Theta_g) \quad (12)$$

$$R_{air} = 0.5 * \rho_{air} * C_D * A_f * v^2 \quad (13)$$

$$R_G = w * \sin(\Theta_g) \quad (14)$$

Where f_r is rolling resistance coefficient, Θ_g is gradient, ρ_{air} is the air density, C_d coefficient of drag, A_f projected area. The lateral forces acting on the front and rear tires are obtained from the linear tire model and are expressed by:

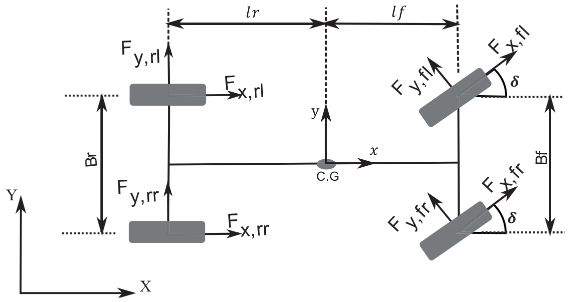

Fig. 3. Schematic of 3DOF vehicle dynamic model.

$$F_{yf} = 2C_{\alpha f}\alpha_f \quad (15)$$

$$F_{yr} = 2C_{\alpha r}\alpha_r \quad (16)$$

Where $C_{\alpha f}$, $C_{\alpha r}$ are the front and rear tire cornering stiffness. $\boldsymbol{\alpha}_f$ and $\boldsymbol{\alpha}_r$ are front and rear slip angles and are computed as follows for small slip angles assumption:

$$\alpha_f = \delta_f - \frac{lf * \omega_z + v_y}{v_x} \quad (17)$$

$$\alpha_r = \frac{lr * \omega_z - v_y}{v_x} \quad (18)$$

the longitudinal wheel forces obtained from linear tire model and computed as follows:

$$F_x = C_i . i \quad (19)$$

Where C_i is longitudinal tire stiffness. i is the tire slip and is defined as:

$$i_i = \begin{cases} \dfrac{\omega_i * r_w - v_x}{\omega_i * r}, & \omega_i * r > v_x \ (Driving) \\ \dfrac{\omega_i * r_w - v_x}{v_x}, & \omega_i * r < v_x \ (Braking) \end{cases} \quad (20)$$

There are 2 control inputs to the vehicle model (u) in equation (21) and the state vector (x) presented in equation (22):

$$u = [\boldsymbol{\omega}, \boldsymbol{\delta}]^T \quad (21)$$

$$x = [X, Y, \Theta, V_x, V_y, \boldsymbol{\omega_z}]^T \quad (22)$$

Where $\boldsymbol{\omega}$ is wheel rotational speed, (*X, Y*) vehicle position, Θ yaw angle, V_x longitudinal velocity, V_y Lateral velocity, $\boldsymbol{\omega}_z$ yaw rate.

The vehicle dynamic model is validated based on [20]. The bicycle model can be used as it matches the response of the proposed model, as shown in Fig. 4,5.

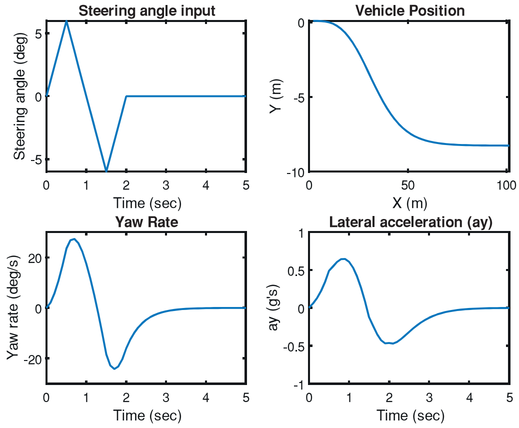

Fig. 4. Vehicle response at Vx=10 m/s.

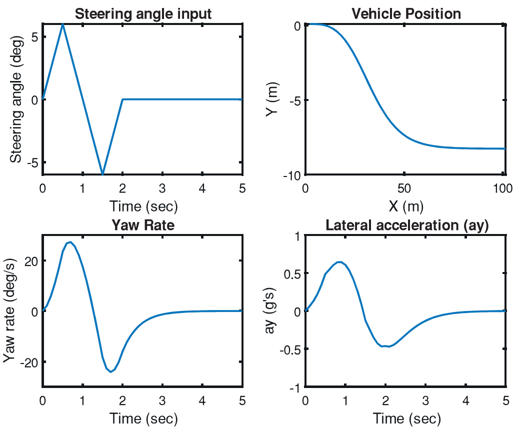

Fig. 5. Vehicle response at Vx=20 m/s.

IV. Simulation Results

Simulation is carried out on a MATLAB environment for the proposed obstacle avoidance algorithm. All vehicle parameters used in this study are in Table 1. Simulations are carried out in scenarios. Case 1 is for avoiding static obstacles, moreover, case 2 concerns moving obstacles. Concerning case 1 three-obstacles are detected the algorithm generates two paths for each obstacle for right and left maneuvers besides, two additional paths involving minimum Euclidean distances for all obstacles. Hence generating 8 paths (Np where p $\in$ [1:8]), As shown in Fig. 6. The curvature of each path for left lane maneuvers are shown in Fig. 7.

The path is terminated if a collision occurs, or the vehicle-to-vehicle distance is less than the safety distance and the remaining paths are assessed based on safety, path length, and smoothness. The optimal path is achieved by minimizing the cost function. As shown in Fig. 8. the optimized path maximum curvature is reduced to 0.105 compared to the original path max curvature of 0.235, enhancing the lateral acceleration and comfortability. the optimization parameters for sigmoid function parameters from the simulation results are in Table 2.

Table 1. Vehicle data for simulation.

m	1280	kg	A_f	2.1	m^2
I_z	2500	$Kg.m^2$	C_d	0.32	
l_f	1.203	m	C_α	30000	N/rad
l_r	1.217	m	C_i	50000	N/unit slip
B_f	1.33	m	μ	0.85	
B_r	1.34	m	r_w	0.3	m

Table 2. Sigmoid function optimization parameters.

Parameter	value
C	0.3450
S	3.7805
Sm	9.5399

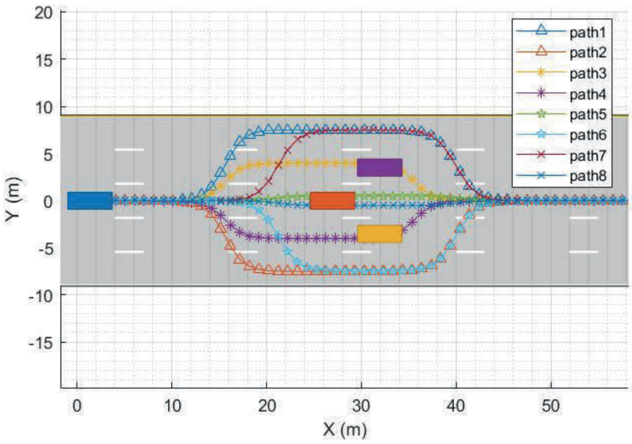

Fig. 6. Generated paths to perform vehicle overtake maneuvers.

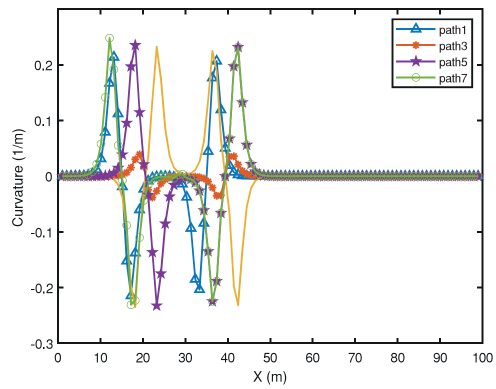

Fig. 7. Curvature for left lane maneuvers.

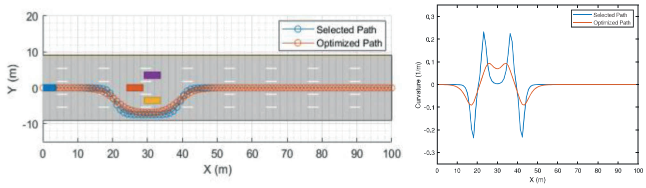

Fig. 8. The curvature of selected and optimized path from the Genetic Algorithm.

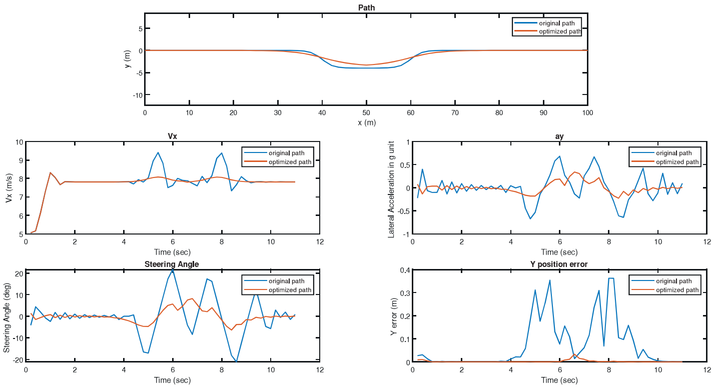

Fig. 9. Vehicle response before and after optimization for static obstacles.

Fig. 9. represents the selected path, the steering input, longitudinal vehicle velocity, lateral acceleration, and The maximum lateral error (Y_{error}) before and after optimization for case 1.

The results reveal that the optimized path satisfies the vehicle-to-vehicle safety distance with avoiding the collision. Further, the path is smooth compared to the original path. The tracking algorithm is followed effectively. Nevertheless, the steering input for the optimized path is sharply decreased compared to the original path, which decreases the steering input by 30.4%. The lateral acceleration for the optimized path is reduced by 44.27% to 0.28g compared to 0.63g before optimization, ensuring the passengers' comfort and reducing vehicle side slip during maneuvers. Y_{error} is significantly reduced by approximately 85% to 0.03 m compared to 0.35 m before optimization, as shown in Fig. 9.

Furthermore, for case 2 the algorithm avoids collisions with the moving obstacles, as shown in Fig. 10,11. The numbers along the paths indicate the number of time steps that ensure a safe distance between the Ego-vehicle and obstacles along the path.

The results for case 2 show that the steering input for the optimized path is reduced by 28%. The lateral acceleration is reduced by 50% to 0.26 g compared to 0.52 g before optimization. Correspondingly, Y_{error} is reduced by 20%, as illustrated in Fig. 12.

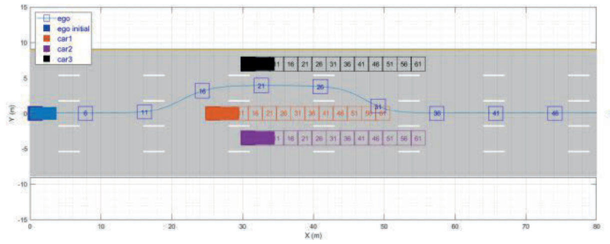

Fig. 10. Ego-Vehicle position before optimization for moving obstacles.

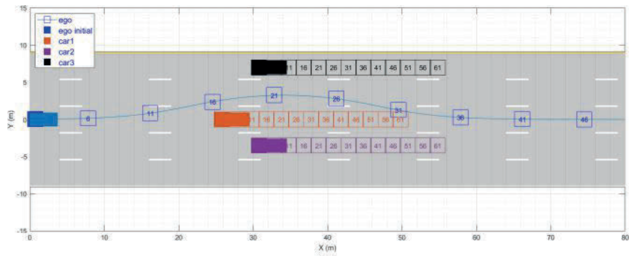

Fig. 11. Ego-Vehicle position after optimization for moving obstacles.

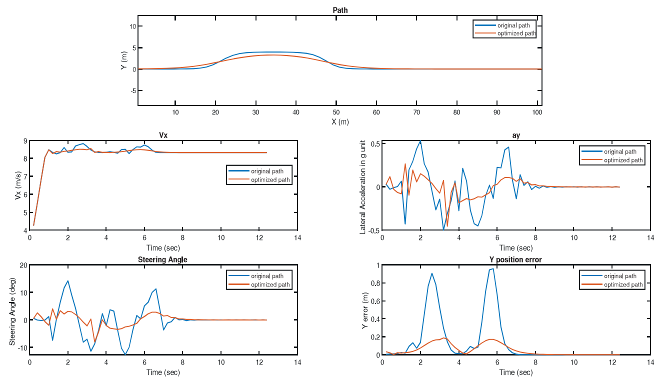

Fig. 12. Vehicle response before and after optimization for moving obstacles.

Currently, the proposed algorithm will be implemented experimentally to a multi-passenger electric golf cart shown in Fig. 13. The vehicle involves an IMU VN-100 and Garmin GPS 18x and Blackfly SU3 camera, which are used in the perception and the localization stages, besides a Velodyne LiDAR VLP-16 sensor for mapping and obstacles detection. Obstacles location, as well as localization data, will be the inputs for the proposed approach, and the algorithm utilized and finds the safe collision-free path and tracking algorithm gives the steering and traction inputs for the low-level control to follow the generated path effectively

Fig. 13. autonomous multi-passenger golf cart research platform

V. CONCLUSION

This paper proposed an obstacle avoidance algorithm for autonomous driving with the avoidance of static and moving obstacles. The proposed algorithm deal with single or multi-vehicle with low computational time. Selecting the best path is based on a cost function that considers safety, path length and smoothness costs and the weights are set to 0.5, 0.3, and 0.2, respectively. This function inhibits the Ego-vehicle from moving close to obstacles and ensure comfortable driving. The best values for sigmoid function parameters are predefined in this paper. The NMPC controller based on the 3DOF vehicle dynamic model used for path tracking is feasible with appropriate performance, and the results demonstrate that lateral acceleration reduced by 44.27% and 50% furthermore, the steering input reduced by 30.4% and 28% for static and dynamic scenarios, respectively

REFERENCES

[1] World Health Organization, 2018. Global status report on road safety 2018. Geneva: World Health Organization. ISBN 978-92-4-156568-4.

[2] Wang, Z., Zlatanova, S. and van Oosterom, P., 2017. Path planning for first responders in the presence of moving obstacles with uncertain boundaries. IEEE Transactions on Intelligent Transportation Systems, 18(8), pp.2163-2173.

[3] Kala, R. and Warwick, K., 2013. Multi-level planning for semi-autonomous vehicles in traffic scenarios based on separation maximization. Journal of Intelligent & Robotic Systems, 72(3), pp.559-590.4

[4] Bry, A. and Roy, N., 2011, May. Rapidly-exploring random belief trees for motion planning under uncertainty. In 2011 IEEE international conference on robotics and automation (pp. 723-730). IEEE.

[5] Karaman, S., Walter, M.R., Perez, A., Frazzoli, E. and Teller, S., 2011, May. Anytime motion planning using the RRT. In 2011 IEEE International Conference on Robotics and Automation (pp. 1478-1483). IEEE.

[6] González, D., Pérez, J., Milanés, V. and Nashashibi, F., 2015. A review of motion planning techniques for automated vehicles. IEEE Transactions on Intelligent Transportation Systems, 17(4), pp.1135-1145.

[7] Petrov, P. and Nashashibi, F., 2014. Modeling and nonlinear adaptive control for autonomous vehicle overtaking. IEEE Transactions on Intelligent Transportation Systems, 15(4), pp.1643-1656.

[8] Pérez, J., Godoy, J., Villagrá, J. and Onieva, E., 2013, May. Trajectory generator for autonomous vehicles in urban environments. In 2013 IEEE international conference on robotics and automation (pp. 409-414). IEEE.

[9] Abdelwahab, M., Parque, V. and El-Bab, A.F., 2019, March. On path planning using minimal aesthetic b-spline curves. In 2019 IEEE 1st Global Conference on Life Sciences and Technologies (LifeTech) (pp. 21-25). IEEE.

[10] Hu, X., Chen, L., Tang, B., Cao, D. and He, H., 2018. Dynamic path planning for autonomous driving on various roads with avoidance of static and moving obstacles. Mechanical Systems and Signal Processing, 100, pp.482-500.

[11] Huy, Q., Mita, S., Nejad, H.T.N. and Han, L., 2013. Dynamic and safe path planning based on support vector machine among multi moving obstacles for autonomous vehicles. IEICE TRANSACTIONS on Information and Systems, 96(2), pp.314-328.

[12] Ben-Messaoud, W., Basset, M., Lauffenburger, J.P. and Orjuela, R., 2018, September. Smooth obstacle avoidance path planning for autonomous vehicles. In 2018 IEEE International Conference on Vehicular Electronics and Safety (ICVES) (pp. 1-6). IEEE.

[13] Huang, X., Zhang, W. and Li, P., 2019. A path planning method for vehicle overtaking manoeuvre using sigmoid functions. IFAC-Papers Online, 52(8), pp.422-427.

[14] AbdElmoniem, A., Osama, A., Abdelaziz, M. and Maged, S.A., 2020. A path-tracking algorithm using predictive Stanley lateral controller. International Journal of Advanced Robotic Systems, 17(6), p.1729881420974852.

[15] Dawood, M., Abdelaziz, M., Ghoneima, M. and Hammad, S., 2020, February. A nonlinear model predictive controller for autonomous driving. In 2020 International Conference on Innovative Trends in Communication and Computer Engineering (ITCE) (pp. 151-157). IEEE.

[16] Abdelwahab, M., Parque, V., Elbab, A.M.F., Abouelsoud, A.A. and Sugano, S., 2020. Trajectory tracking of wheeled mobile robots using Z-number based fuzzy logic. IEEE Access, 8, pp.18426-18441.

[17] Ibrahim, F., Abouelsoud, A.A., Fath Elbab, A.M. and Ogata, T., 2019. Path following algorithm for skid-steering mobile robot based on adaptive discontinuous posture control. Advanced Robotics, 33(9), pp.439-453.

[18] Lian, J., Yu, W., Xiao, K. and Liu, W., 2020. Cubic Spline Interpolation-Based Robot Path Planning Using a Chaotic Adaptive Particle Swarm Optimization Algorithm. Mathematical Problems in Engineering, 2020.

[19] Wong, J.Y., 2008. Theory of ground vehicles. John Wiley & Sons.

[20] Liu, W., He, H. and Sun, F., 2016. Vehicle state estimation based on minimum model error criterion combining with extended Kalman filter. Journal of the Franklin Institute, 353(4), pp.834-856.

[21] Smith, D.E. and Starkey, J.M., 1995. Effects of model complexity on the performance of automated vehicle steering controllers: Model development, validation, and comparison. Vehicle system dynamics, 24(2), pp.163-181.